

Fabrication and Characterization of Al₂O₃-Cu Composites Prepared by Uniaxial Pressing

Paulina Piotrkiewicz¹, Justyna Zygmuntowicz^{1*}, Marcin Wachowski², Ireneusz Szachogluchowicz², Waldemar Kaszuwara¹, Joanna Szymańska³

¹Warsaw University of Technology, Faculty of Materials Science and Engineering, 141 Woloska St., 02-507 Warsaw, Poland

²Military University of Technology, Faculty of Mechanical Engineering, 2 gen. S. Kaliskiego St., 00-908 Warsaw, Poland

³Imerys Technology Center, 1 rue Le Chatelier, 38090 Vaulx-Milieu, France

<https://doi.org/10.62753/ctp.2026.02.2.2>

Abstract

This study evaluates the fabrication and performance of Al₂O₃-Cu composites containing 10 vol.% Cu produced by uniaxial pressing (100 MPa) and free sintering in 95% Ar/5% H₂ at 1200–1400°C. A strong temperature–densification relationship was observed. The relative density increased from 81.44% at 1200°C to 97.32% at 1400°C, while the open porosity decreased from 18.27% to 0.15%. Water absorption was reduced from 4.76% to 0.04%, confirming near-complete pore elimination at 1400°C. XRD analysis identified only α -Al₂O₃ and Cu phases, with no secondary reaction products. SEM observations revealed irregular copper agglomerates formed by liquid-phase migration; however, no macroscopic exudation was detected, indicating effective capillary retention of molten Cu (melting point 1085°C). EDS confirmed sharp phase boundaries without interdiffusion. The optimally sintered composite (1400°C) exhibited a Vickers hardness of 11.7 ± 0.9 GPa and an apparent indentation fracture toughness of 5.90 ± 1.80 MPa·m^{0.5}. Grain-size analysis showed a fine, unimodal alumina distribution predominantly within 0.6–1.2 μ m. Digital image correlation during compression revealed heterogeneous strain localization governed by phase distribution. The results demonstrate that dense, mechanically reliable Al₂O₃-Cu composites can be fabricated via a scalable, cost-effective powder metallurgy route.

Keywords: uniaxial pressing, Al₂O₃-Cu, composites, copper

Introduction

The development of multifunctional ceramic–metal composites remains a central challenge in contemporary materials engineering. Structural ceramics such as Al₂O₃ offer high hardness, excellent wear resistance, chemical stability, and superior high-temperature performance; however, their intrinsic brittleness significantly limits their reliability under complex mechanical loading [1–4]. Conversely, metals exhibit high

ductility and energy absorption capacity but lack the stiffness, hardness, and thermal stability required in demanding environments. The deliberate combination of these two material classes into a single composite system provides a pathway toward synergistic property enhancement that cannot be achieved by either phase alone.

Among ceramic-metal systems, Al_2O_3 -Cu composites represent a particularly attractive material platform. Alumina provides a rigid, thermally stable matrix, while copper introduces ductility, high thermal conductivity, and high electrical conductivity [5-7]. Despite this apparent complementarity, the processing of Al_2O_3 -Cu materials is nontrivial. The relatively low melting point of copper [8-10] and its high contact angle on alumina lead to non-wetting liquid-phase sintering conditions [11-15], which may promote phase migration, agglomeration, or microstructural heterogeneity. As a result, controlling densification, phase distribution, and interfacial stability remains a key issue in the fabrication of such composites.

Most studies on ceramic-metal composites focus on advanced consolidation techniques, such as hot pressing [15-17], the plasma-electrolytic oxidation method [18-19], spark plasma sintering [20-21], and pressure-assisted sintering [22-23], which enable improved densification but increase the technological complexity and production costs. In contrast, conventional uniaxial pressing followed by free sintering remains an industrially scalable and economically viable route, particularly for components with relatively simple geometries. Nevertheless, the applicability of this method to Al_2O_3 -Cu systems with a significant volume fraction of the metallic phase requires detailed verification, particularly regarding densification behavior, liquid-phase stability, and mechanical performance.

The present work addresses this technological gap by systematically investigating Al_2O_3 -Cu composites containing 10 vol.% Cu fabricated via uniaxial pressing and free sintering under a reducing atmosphere. This composite was chosen owing to the specific properties of the components used to produce it.

Alumina is a widely used structural ceramic due to its high hardness, compressive strength, wear resistance, and high elastic modulus (~ 380 GPa) [24-26]. It also exhibits excellent thermal stability (melting point $\sim 2050^\circ\text{C}$), chemical inertness, and oxidation resistance, making it suitable for demanding environments [27-28]. Nonetheless, its relatively low fracture toughness ($3\text{-}5 \text{ MPa}\cdot\text{m}^{0.5}$) limits reliability under tensile or impact loading [29], necessitating the incorporation of a ductile phase to improve damage tolerance.

Copper was selected as the metallic component because of its high plastic deformability, energy absorption capacity, as well as excellent thermal and electrical conductivity ($\sim 401 \text{ W/m}\cdot\text{K}$) [32-34]. It enhances fracture resistance through mechanisms such as crack bridging, deflection, and plastic deformation at the crack tip [30-31], thereby reducing stress concentrations and improving resistance to brittle failure. This also enables the development of multifunctional materials combining mechanical integrity with efficient heat and charge transport.

From a processing standpoint, the Al_2O_3 -Cu system is well suited for uniaxial pressing. Alumina ensures dimensional stability during compaction, while ductile copper particles improve the packing density and interfacial contact. The lower melting point of copper (1085°C) [35] facilitates liquid-phase-assisted densification without compromising the ceramic matrix. Additionally, the chemical compatibility between Al_2O_3 and Cu under controlled conditions supports microstructural stability.

The Al_2O_3 -Cu system provides a synergistic combination of mechanical strength, fracture toughness, and functional properties, making it suitable for the cost-effective fabrication of multifunctional composites via conventional powder metallurgy routes. The combination of alumina and copper thus provides a synergistic balance of properties. The ceramic phase provides hardness, stiffness, and environmental resistance, while the metallic phase enhances the fracture toughness, thermal conductivity, and energy absorption. This complementary interaction makes the Al_2O_3 -Cu system particularly suitable for shield-type composite components produced by conventional powder metallurgy techniques such as uniaxial pressing. The decision to employ Al_2O_3 as the ceramic matrix and Cu as the metallic phase was driven by their complementary mechanical and functional properties, compatibility with uniaxial pressing, and suitability for scalable, cost-effective manufacturing. The resulting composite system offers a combination of structural performance and multifunctional characteristics that cannot be achieved in monolithic ceramic materials.

A key contribution of this study lies in the comprehensive correlation between the processing temperature, densification efficiency, phase stability, microstructural evolution, and mechanical response. By analyzing four sintering temperatures in the range of 1200 - 1400°C , the study identifies the critical temperature conditions necessary to achieve near-full densification while maintaining phase integrity and preventing macroscopic metallic exudation.

In addition to conventional density and phase analysis, the work introduces full-field strain monitoring using digital image correlation during monotonic compression testing. This approach provides detailed insight into strain localization, phase interaction, and failure mechanisms, extending beyond standard mechanical characterization. The integration of stereological grain-size analysis further enables the assessment of microstructural stability and grain growth control in the presence of a liquid metallic phase.

From a materials engineering perspective, the study demonstrates that high-density Al_2O_3 -Cu composites with a controlled microstructure can be successfully produced using a cost-effective uniaxial pressing route, despite the challenges associated with non-wetting liquid-phase sintering. The results contribute to a better understanding of the capillary retention of liquid copper within an alumina skeleton, the effects of phase distribution on strain localization, in addition to the relationship between densification and mechanical reliability.

By combining scalable processing, detailed microstructural analysis, and advanced mechanical characterization, this work provides both scientific insight and practical guidance for the design of ceramic-

metal composites for structural and multifunctional applications, including shielding components, thermally loaded elements, and applications in mechanically demanding environments.

Materials and methods

The selection of the constituent phases for the fabrication of the ceramic-metal composites by uniaxial pressing was based on a comprehensive evaluation of the mechanical performance, functional characteristics, processing compatibility, and economic feasibility. In the present study, alumina (TM-DAR, Taimei Chemicals, Japan) was chosen as the ceramic matrix, while copper (Sigma-Aldrich) was introduced as the ductile metallic component.

The composites were fabricated by uniaxial pressing following a multistep powder preparation route designed to ensure adequate homogenization and processability of the Al_2O_3 -Cu mixture. In the first stage, the alumina and copper powders were combined in the required proportions and mechanically mixed to achieve a macroscopically uniform distribution of both phases. The components were homogenized using ethyl alcohol as the solvent in a Retsch PM400 planetary ball mill, in a corundum container, for 1 hour at 300 rpm. The 6 corundum grinding media were used for mixing. The obtained mass was dried in a laboratory dryer at 45°C for 48 hours, followed by the gradual addition of a binder solution for the powders. The solution was added incrementally under continuous mixing to promote uniform coating of both the ceramic and metallic particles as well as to facilitate the formation of granules with sufficient mechanical integrity. The selection of the type of binder and its content was based on prior studies [36-37], ensuring an optimal balance between green strength and processability. Following binder addition, the moist powder mixture was granulated by sieving through meshes with apertures of $600\ \mu\text{m}$, $400\ \mu\text{m}$, and $150\ \mu\text{m}$. This step resulted in the formation of irregular but relatively cohesive granules with a controlled size distribution. The granules exhibited good flowability and packing ability, which are critical for uniform die filling during uniaxial pressing. At the same time, the granulation process primarily affected the powder mixture's agglomeration state and did not alter the intrinsic morphology or size of the copper particles. The resulting granulated feedstock enabled improved compaction behavior and enhanced homogeneity of the green bodies prior to sintering.

The actual density of the composite mixture used to form the composites was $4.522 \pm 0.037\ \text{g/cm}^3$. This value was determined by means of a helium pycnometer. The pressing process was carried out utilizing a hydraulic press. A sintered carbide matrix with a 20 mm diameter was employed to form the shapes. The pressing pressure was 100 MPa each time. Four series of composite samples from the Al_2O_3 -Cu system were produced. Each of the produced series differed in sintering temperature. The content of the metallic phase was 10% by volume. The raw shapes of each series were then subjected to free-form sintering. The sintering process was carried out in a Nabertherm RHTC 80-230/16 tube furnace in a reducing atmosphere (95% Ar/5% H_2). The use of a reducing atmosphere was intended to prevent the formation of spinel structures and the oxidation of copper and other metallic components during sintering. Due to the low melting point of copper, which

remains liquid during sintering, and the high contact angle between pure copper and aluminum oxide, the sintering of the composite samples was characterized as sintering with a non-wetting liquid phase [38]. Four sintering temperatures were applied: 1200°C (Series I), 1250°C (Series II), 1300°C (Series III), and 1400°C (Series IV). The temperatures were selected so that the highest was the sintering temperature, enabling the formation of high-density solid ceramic-metal composites based on Al₂O₃ [39]. The use of lower temperatures was intended to determine whether the process temperature could be reduced. The sintering procedure remained the same for each sintering temperature. Heating was carried out in three stages: from 20°C to 120°C at 5°C/min, from 120°C to 750°C at 1°C/min, and from 750°C to the sintering temperature at 2°C/min. The sintering time for each temperature was 2 hours. The system was then cooled at 4°C/min until it reached ambient temperature.

The physical properties of the Al₂O₃-Cu composites were determined using the Archimedes immersion method. The measurements were conducted in accordance with standard procedures for sintered materials, based on mass determination in air and in a liquid of a known density (distilled water). Prior to testing, the specimens were dried to a constant mass to eliminate the influence of residual moisture. Subsequently, each sample was weighed in air, immersed in water to determine the apparent immersed mass, and then weighed in the saturated state after surface drying.

The Archimedes method enables a reliable assessment of the densification efficiency and pore structure in ceramic-metal composites. For Al₂O₃-Cu materials, the measured densities provide indirect information on the effectiveness of particle packing during uniaxial pressing and the degree of sintering. At the same time, the apparent porosity reflects the extent of residual open-pore networks, which may influence the mechanical strength, thermal conductivity, and overall functional performance.

Phase identification was performed by X-ray diffraction analysis with Cu K α radiation ($\lambda = 1.5406 \text{ \AA}$). Diffraction patterns were recorded over an appropriate 2θ range with a constant step size and counting time to ensure sufficient peak resolution. The obtained diffractograms were analyzed by comparison with reference data from crystallographic databases.

A preliminary evaluation of the surface topography and distribution of the metallic phase within the composite was performed employing confocal laser scanning microscopy. Observations were performed by means of an Olympus LEXT OLS4100 microscope, which enabled non-contact, high-resolution surface imaging. This stage of analysis provided qualitative insight into the surface morphology of the sintered specimens and the spatial arrangement of the metallic constituent within the composite structure.

Comprehensive microstructural characterization was subsequently conducted by scanning electron microscopy (SEM). Both polished sections and fracture surfaces were examined utilizing a JEOL JSM-6610 operating at 15 kV. Imaging was performed in secondary electron (SE) mode to assess the surface morphology and in backscattered electron (BSE) mode to enhance the compositional contrast between the ceramic matrix

and the metallic phase. To eliminate charging effects during SEM analysis, all the specimens were coated with a thin conductive carbon layer using a JEOL Fine Coat Ion Sputter JFC-1100 prior to examination.

The chemical composition and phase distribution of the Al_2O_3 -Cu composites were analyzed by energy-dispersive X-ray spectroscopy (EDS) integrated with a scanning electron microscope (SEM). The analysis was performed at an accelerating voltage of 15 kV, which ensured sufficient excitation of characteristic X-ray lines for both the metallic and ceramic elements while maintaining adequate spatial resolution. Elemental mapping was conducted in a semi-quantitative mode without the use of external standards, and the results were interpreted qualitatively to identify the phase distribution as well as interfacial characteristics. The typical acquisition time is 120 s per analyzed area, providing an acceptable signal-to-noise ratio for reliable elemental detection and mapping. It should be noted that EDS analysis has inherent limitations, particularly in the detection and quantification of light elements such as oxygen. The measured oxygen signal should therefore be interpreted with caution since it may be affected by factors such as absorption effects, detector efficiency, and interaction volume. Furthermore, the spatial resolution of EDS is limited by the electron interaction volume, especially at the applied accelerating voltage, potentially leading to signal overlap at the phase boundaries. Consequently, the EDS results presented in this study are intended primarily to confirm the qualitative distribution of Al, O, and Cu in addition to assess the presence or absence of secondary phases at the micrometer scale. While no additional phases or reaction products were detected within the method's resolution limits, it cannot be excluded that very thin interfacial layers or nanoscale reactions may have remained undetected.

Mechanical characterization included Vickers hardness testing conducted on polished, parallel surfaces prepared according to standard metallographic procedures. Indentations were performed by means of an HVS-30T hardness tester under a constant load of 98 N applied for 15 s. These parameters were maintained for all the specimens to ensure reproducibility and comparability across the sample series.

The resistance of the Al_2O_3 -Cu composites to brittle fracture was evaluated employing the indentation fracture method. Fracture toughness was estimated according to the relationship proposed by Lankford [40], which is applicable to various crack geometries associated with Vickers indentation. Radial crack lengths extending from the corners of the indentation imprints produced under a load of 98 N were measured and used for calculations. For statistical reliability, ten indentations were made in each specimens, including those of the composites fabricated using different temperatures.

The mechanical response of the sintered Al_2O_3 -Cu composites was further characterized by monotonic compression testing. The purpose of this experimental series was to determine the compressive strength of the materials as well as to examine their deformation and failure behavior using full-field strain analysis based on digital image correlation (DIC).

The mechanical behavior of the Al_2O_3 -Cu composites under compressive loading was evaluated by means of uniaxial compression tests performed under controlled conditions. The tests were carried out on

cylindrical specimens with a diameter of 20 mm and a height of approximately 10 mm, corresponding to a height-to-diameter ratio (H/D) of ~ 0.5 . This geometry was selected to ensure stable loading conditions and to minimize the risk of buckling, while maintaining comparability with standard testing practices for brittle materials. Prior to testing, the specimen end surfaces were carefully ground and polished to achieve parallelism and planarity, which are critical for uniform stress distribution during compression. The final surface preparation step involved fine polishing to eliminate surface irregularities and reduce stress concentrations at the contact interfaces. The parallelism of the loading faces was controlled to within a tight tolerance to avoid bending stresses during testing. Compression experiments were conducted using a servo-hydraulic testing machine under displacement-controlled conditions. A constant crosshead speed of 0.5 mm/min was applied, corresponding to a nominal strain rate on the order of 10^{-3} 1/s, which is appropriate for the quasi-static testing of ceramic materials. The load and displacement were continuously recorded throughout the test until catastrophic failure. To reduce the frictional effects between the specimen and the loading platen, the contact surfaces were carefully aligned, and, where necessary, a thin layer of lubricant or a compliant interlayer was applied to improve load transfer. All the tests were performed at ambient temperature under laboratory conditions. For statistical reliability, multiple specimens from each series were tested, and the reported mechanical parameters represent average values. This detailed methodology ensures reproducibility of the results and enables a reliable interpretation of the compressive behavior of the investigated ceramic-metal composites.

Full-field strain distribution and deformation evolution were monitored by a Dantec Q400 DIC system equipped with two 8-megapixel cameras. The system provided a displacement measurement accuracy of ± 0.01 pixels and a strain resolution of 0.01%. Data acquisition and post-processing were performed utilizing ISTR4 4D software, which enabled both visualization of the strain fields and detailed quantitative analysis of local deformation. The applied monotonic compressive loading allowed the force-displacement characteristics to be determined for each specimen. All the tests were conducted under controlled laboratory conditions at $22 \pm 2^\circ\text{C}$. To ensure statistical reliability, eight specimens from each material series were examined. The results presented in the subsequent section include averaged force-displacement curves and representative DIC strain maps for each composite group.

In addition, the grain size of the Al_2O_3 ceramic matrix was quantified employing stereological analysis. Fracture surfaces were observed by scanning electron microscopy, and individual alumina grains were manually delineated, accounting for their three-dimensional morphology. Digital image processing techniques were applied to identify the grain boundaries and generate binary images suitable for quantitative evaluation. The analysis was conducted using Micrometer software [41-43], which enabled calculation of the average equivalent grain diameter (d_2). Parameter d_2 corresponds to the diameter of a circle having an area equal to that of the measured irregular grain [41-42]. Based on the obtained measurements, percentage distributions of equivalent grain diameters were established for all the investigated composites. To ensure statistical

significance, SEM micrographs were randomly selected, and no fewer than 1000 individual grains were measured for each composite, including specimens of the composites produced using different temperatures. This procedure provided a representative description of the grain-size distribution within the ceramic matrix and enabled correlation of the microstructural features with the observed mechanical behavior.

Results

Figure 1 shows the morphology of the starting powders used to fabricate the samples. In Figure 1a) a scanning electron micrograph of the alumina powder (TM-DAR, Taimei Chemicals, Japan) is shown. The powder consists of fine, nearly spherical primary particles with submicron sizes (typically below 1 μm) that form agglomerates. The high degree of agglomeration is characteristic of ultrafine ceramic powders and results from strong interparticle forces. The relatively uniform particle size distribution and rounded morphology are beneficial for achieving a high packing density and homogeneous microstructure during forming and sintering. Figure 1b) presents SEM micrographs of the copper powder (Sigma-Aldrich) at two magnifications. The powder exhibits a heterogeneous morphology, consisting of irregular, plastically deformed particles with a broad size distribution ranging from several to tens of micrometers. Many particles exhibit flattened or elongated shapes, along with surface roughness indicative of mechanical processing. The presence of agglomerates and interparticle contacts is also observed. Such morphology promotes mechanical interlocking and plastic deformation during uniaxial pressing, but may also contribute to inhomogeneous distribution and the formation of metallic agglomerates in the composite.

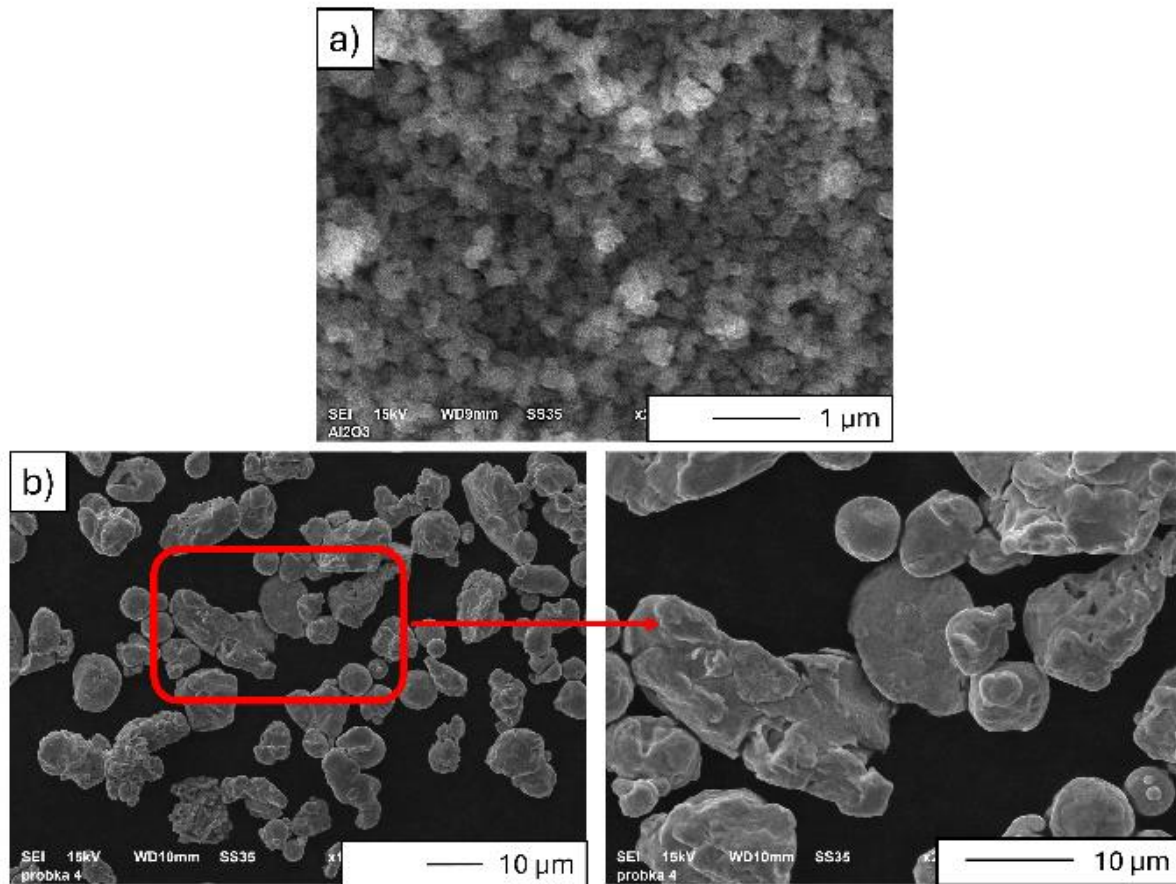


Figure 1. Morphology of starting powders used to fabricate $\text{Al}_2\text{O}_3\text{-Cu}$ composites: a) alumina, b) cooper.

The starting powders used in this study are characterized by high purity to minimize the influence of impurities on the phase stability, sintering behavior and interfacial interactions in the $\text{Al}_2\text{O}_3\text{-Cu}$ system. The alumina powder (TM-DAR, Taimei Chemicals, Japan) is a high-purity $\alpha\text{-Al}_2\text{O}_3$ grade, typically characterized by a purity exceeding 99.99%. The high chemical purity of TM-DAR alumina ensures reproducible sintering behavior and limits the formation of undesired secondary phases during thermal treatment.

The copper powder (Sigma-Aldrich) used in this work is of high purity, typically $\geq 99.9\%$, as specified by the manufacturer. The main impurities in commercial copper powders generally include trace amounts of oxygen and minor metallic elements. Under the applied reducing atmosphere (95% $\text{Ar}/5\% \text{H}_2$), the risk of oxide formation is minimized, ensuring that the copper remains predominantly in the metallic state during sintering. The high purity of the metallic phase is particularly important to maintain its ductility, electrical and thermal conductivity, as well as to avoid the formation of interfacial reaction products.

The use of high-purity starting materials in both phases is critical to ensure that the observed microstructural evolution and mechanical properties of the composites result primarily from the processing conditions and phase interactions, rather than from impurity-driven effects.

Attempts to produce composite shapes with a 10% volume fraction of metallic phase by uniaxial pressing with free sintering revealed a clear relationship between sample densification and the sintering temperature. The obtained values of the physical properties are summarized in Table 1. The lowest densification was observed for the Series I samples sintered at 1200°C, with an average relative density of 81.44% of the theoretical density, while the highest densification was observed for Series IV sintered at 1400°C, with an average relative density of 97.32% of the theoretical density. The relative densities of the samples sintered at 1250°C and 1300°C were 87.29% (Series II) and 92.27% (Series III), respectively. Based on the values obtained for each series, it was decided to conduct further tests on Series IV, which exhibited the highest densification.

A systematic decrease in open porosity was observed with increasing sintering temperature. Series I, sintered at 1200°C, exhibited an open porosity of 18.27%. Raising the temperature to 1250°C (Series II) reduced the open porosity to 11.78%. A further decline was recorded for Series III (1300°C), reaching 6.97%, while Series IV, sintered at 1400°C, showed a nearly fully dense structure with an open porosity of only 0.15%.

A similar trend was noted for water absorption. The highest value was measured for Series I (4.76%), followed by Series II (2.92%) and Series III (1.66%).

The lowest water absorption, 0.04%, was obtained for Series IV. The progressive reduction in water absorption directly correlates with a decrease in open porosity, indicating improved densification and pore elimination at higher sintering temperatures. The results clearly demonstrate that increasing the sintering temperature significantly enhances the densification of Al₂O₃-Cu composites produced by uniaxial pressing, resulting in a substantial reduction in both open porosity and water absorption. The nearly complete elimination of open porosity at 1400°C suggests effective particle rearrangement, enhanced diffusion processes, and improved interfacial bonding between the ceramic matrix and the metallic phase. Based on the values obtained for each series, it was decided to conduct further tests only on Series IV (1400°C), which demonstrated the highest densification.

Table 1. Densification parameters of Al₂O₃-Cu composites as a function of sintering temperature.

Series	Sintering temperature [°C]	Relative density [%]	Open porosity [%]	Water absorption [%]	Number of samples tested
I	1200	81.44 ± 1.08	18.27 ± 0.95	4.76 ± 0.54	8
II	1250	87.29 ± 1.02	11.78 ± 0.75	2.92 ± 0.52	
III	1300	92.27 ± 0.85	6.97 ± 0.87	1.66 ± 0.13	
IV	1400	97.32 ± 0.95	0.15 ± 0.09	0.04 ± 0.01	

Figure 2 presents macrographs of the Al₂O₃-Cu composite specimens containing 10 vol.% Cu (Series IV), fabricated by uniaxial pressing followed by free sintering at 1400°C. The specimens exhibit a well-defined geometry and dimensional integrity, indicating that the applied forming pressure (100 MPa) was sufficient to

achieve uniform green-body consolidation prior to sintering. The macroscopic evaluation confirmed that the uniaxial pressing route enables the successful fabrication of composites with a relatively high metallic phase content (10 vol.%) without visible structural defects such as edge cracking, delamination, or distortion. The surfaces of the sintered specimens appear homogeneous and compact, with no visible metallic exudation or surface segregation. Importantly, no crystallized or segregated metallic phase was observed on the specimen surfaces. This suggests that, despite the presence of copper, which has a significantly lower melting point (1085°C) than the applied sintering temperature, the metallic phase remained effectively incorporated into the ceramic matrix during thermal treatment. The absence of copper-rich surface regions indicates that uncontrolled liquid-phase migration or sweating did not occur to a macroscopically detectable extent. This behavior implies good capillary retention of the liquid copper within the Al₂O₃ skeleton and adequate interfacial stability under the applied sintering conditions. The above considerations will be supported by further research presented in the manuscript.

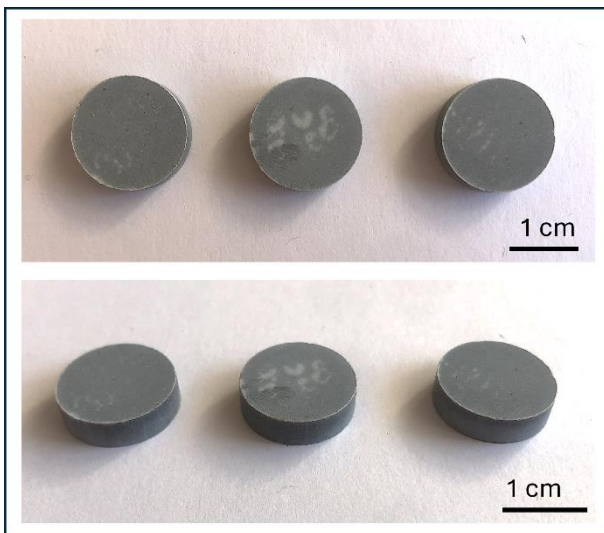


Figure 2. Example photos of Al₂O₃-Cu composite samples with 10 vol.% metallic phase produced by uniaxial pressing and free sintering at 1400°C.

Phase analysis of the specimens from the Al₂O₃-Cu system under uniaxial pressing (Figure 3) did not reveal any new phases. In the uniaxially pressed specimens, reflections corresponding to the Al₂O₃ (#04-015-8994) and Cu (#04-016-6874) crystallographic planes were confirmed. Based on the obtained diffractograms, there was no relationship between the sintering temperature and the material's phase composition.

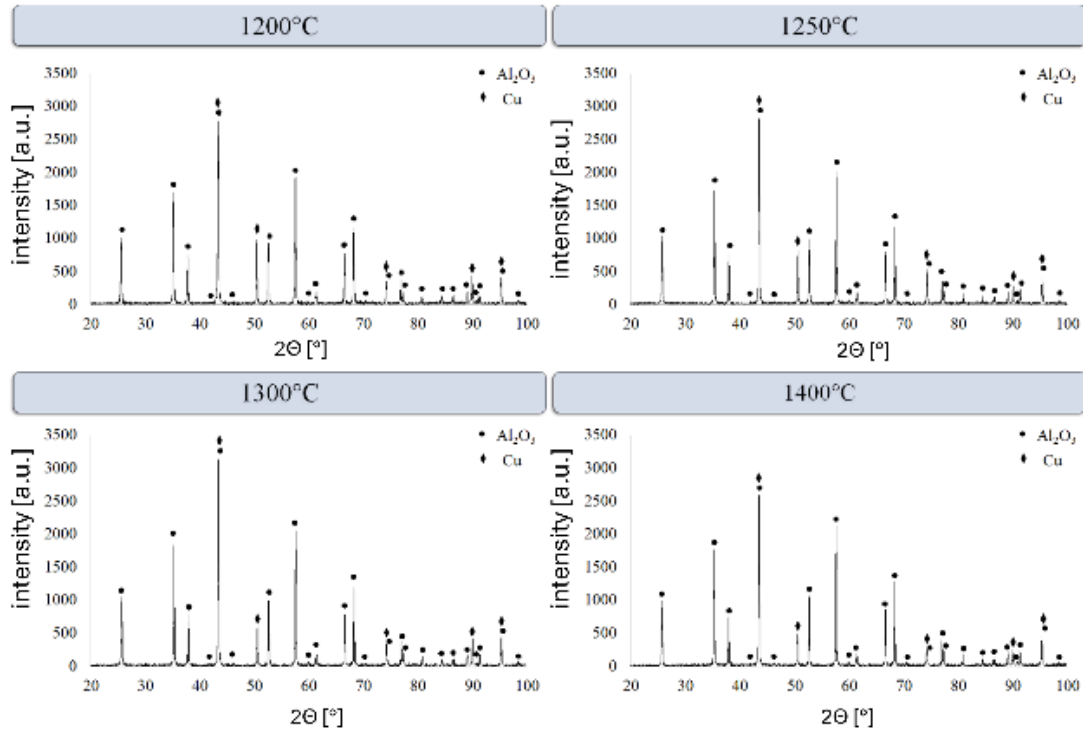


Figure 3. Phase analysis results for all series of produced composites, depending on applied sintering temperature.

In the next step, more detailed observations of the surfaces of the Al₂O₃-Cu samples sintered at 1400°C were made. These observations were made by means of a confocal microscope, which revealed that the surface of the Al₂O₃-Cu specimens (Figure 4) was characterized by numerous metallic particles randomly distributed throughout the matrix. The metallic particles tended to agglomerate into larger clusters. In the central part of the specimen, cavities left by copper particles were observed. Their formation is most likely related to the poor adhesion of the copper particles to the ceramic matrix, which favors both the flow of copper during sintering and the subsequent removal of particles during preparation of the specimens for observation.

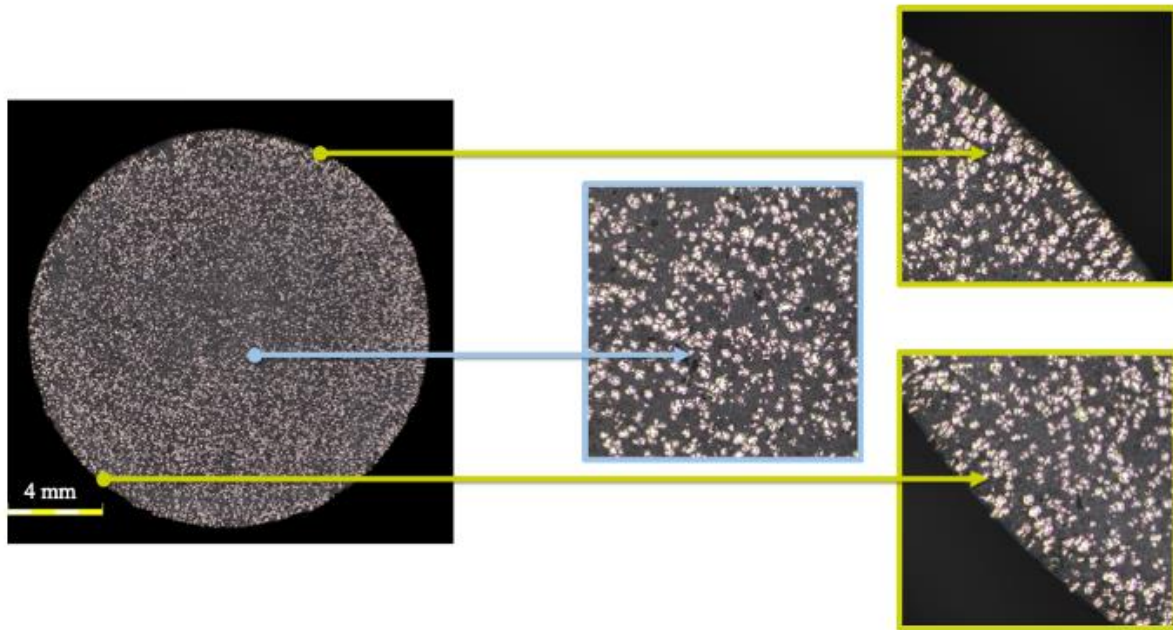


Figure 4. Example micrographs of specimen surfaces from $\text{Al}_2\text{O}_3\text{-Cu}$ system with 10 vol.% metallic phase produced by uniaxial pressing and free sintering at 1400°C .

The SEM micrographs revealed the presence of metallic particles of various sizes, irregularly distributed in the composite (Figure 5). During sintering, the copper particles joined to form larger agglomerates with irregular geometries. Their formation was associated with the migration of liquid copper within the matrix. The moving areas of liquid copper connected upon contact. This meant that the obtained microstructure consisted of both areas with a very high concentration of the metallic phase and areas where metal particles were absent. Such a large variation in the distribution of the metallic phase may lead to nonuniform properties throughout the material volume.

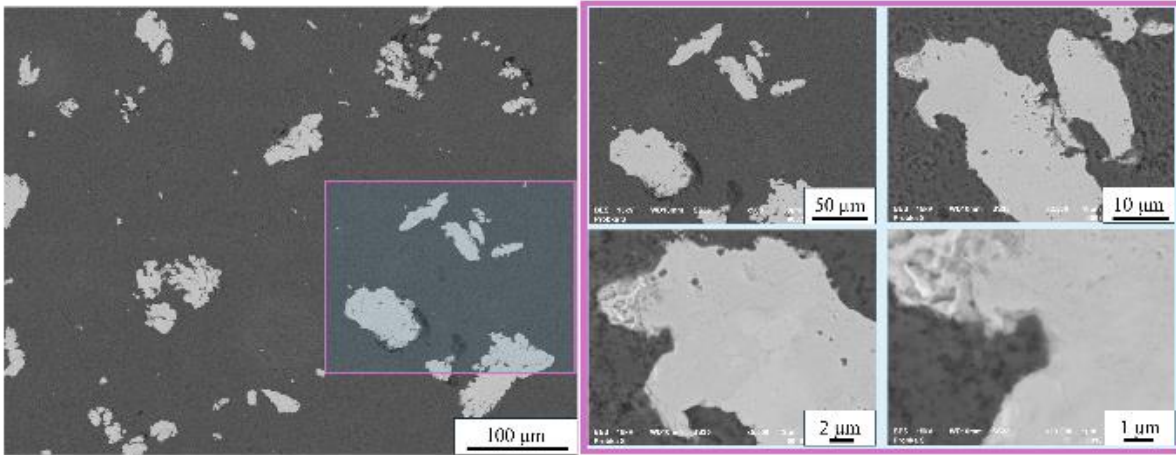


Figure 5. Example SEM micrographs showing microstructure of Al_2O_3 -Cu specimen with 10 vol.% metallic phase produced by uniaxial pressing and free sintering at 1400°C .

Figure 6 presents the results of X-ray microanalysis (SEM-EDS) performed on the Al_2O_3 -Cu composite containing 10 vol.% Cu, fabricated by uniaxial pressing and sintered at 1400°C . The analysis includes a backscattered electron (BSE) micrograph, elemental distribution maps for Al, O, and Cu, and a composite elemental overlay. The BSE micrograph reveals a distinct contrast between the ceramic matrix and the metallic phase. The bright region corresponds to a copper-rich area due to the higher atomic number of Cu relative to Al and O, whereas the darker surrounding matrix corresponds to the Al_2O_3 phase. The metallic phase appears as an irregularly shaped, compact agglomerate embedded within the ceramic matrix.

No evidence of interfacial cracking or debonding is observed at this magnification, suggesting good interfacial integrity after sintering at 1400°C . Elemental mapping confirms the phase distribution identified in the BSE micrograph. The Al and O maps show strong, homogeneous signals in the matrix region, whereas their intensities are significantly reduced within the metallic inclusion. This clearly indicates that the surrounding phase consists of alumina. In contrast, the Cu map shows a high-intensity signal confined to the bright inclusion area, confirming that this region is composed of copper. The sharp compositional boundary between Cu and the Al_2O_3 matrix suggests limited interdiffusion between the phases under the applied sintering conditions. The composite elemental overlay further demonstrates the spatial separation of the metallic and ceramic phases, with copper confined to discrete regions and no detectable Cu dispersion within the alumina matrix. The absence of additional elemental signals indicates that no secondary reaction products or interfacial phases were formed at a detectable level during sintering. The EDS microanalysis confirms a two-phase microstructure consisting of a continuous Al_2O_3 matrix and discrete Cu inclusions, with clear phase boundaries between the components at 1400°C . Moreover, no evidence of a chemical reaction was detected within the resolution limits of the conducted SEM-EDS analysis.

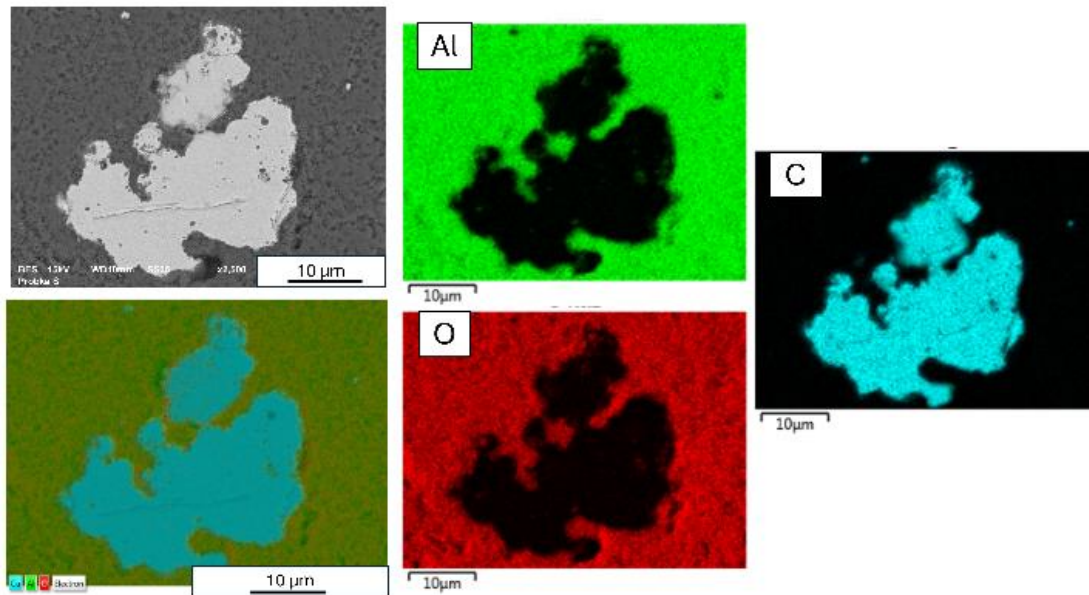


Figure 6. X-ray microanalysis of chemical composition of specimen from Al_2O_3 -Cu system with 10 vol.% metallic phase produced by uniaxial pressing and sintered at 1400°C .

The mechanical properties of the Al_2O_3 -Cu composite containing a 10 vol.% metallic phase, fabricated by uniaxial pressing and sintered at 1400°C , were evaluated by Vickers indentation. The material exhibited an average hardness of 11.7 ± 0.9 GPa. The relatively low standard deviation indicates a fairly homogeneous microstructure at the indentation scale, suggesting a uniform phase distribution and effective densification, consistent with the previously observed negligible open porosity. The fracture toughness, expressed as the indentation fracture toughness coefficient (K_{IC}), was determined to be 5.90 ± 1.80 $\text{MPa}\cdot\text{m}^{0.5}$. The relatively higher scatter in K_{IC} values (± 1.80 $\text{MPa}\cdot\text{m}^{0.5}$) may result from the heterogeneous nature of crack-particle interactions as indentation cracks can intersect copper inclusions to varying degrees depending on their local distribution and size.

The fracture toughness values determined by the indentation method should be regarded as apparent values, strongly influenced by the local microstructure of the Al_2O_3 -Cu composite. Owing to the pronounced heterogeneity of the material, particularly the non-uniform distribution and size of the copper inclusions, crack propagation under Vickers indentation is highly dependent on the local phase arrangement.

When cracks interact with ductile copper particles or agglomerates, mechanisms such as crack deflection, bridging, and local plastic deformation may occur, leading to a reduction in the crack length and, consequently, an increase in the calculated K_{IC} . As a result, indentations located in Cu rich regions may yield elevated toughness values compared to those formed in ceramic-dominated areas.

Furthermore, the indentation method assumes locally homogeneous material behavior, which is not fully satisfied in this composite system. Therefore, the reported K_{IC} values should be interpreted as effective, microstructure-dependent parameters and not as intrinsic material constants. In this context, they represent an upper-bound estimate of the fracture resistance under localized loading conditions.

The load-displacement curve (Figure 7) obtained during uniaxial compression testing of the Al_2O_3 -Cu composite, reveals a mechanical response characteristic of ceramic matrix composites with metal particles. The initial stage of loading is represented by an almost linear relationship between the load and platen displacement, indicating predominantly elastic deformation and effective load transfer within the composite structure. With increasing displacement, a slight deviation from linearity is observed, suggesting progressive accumulation of microstructural damage associated with the initiation of microcracks at the ceramic-metal interfaces and localized plastic accommodation within the copper phase. The material reached a maximum compressive strength of 103.26 MPa at a displacement of approximately 0.4 mm, followed by a rapid drop in load corresponding to catastrophic failure. The abrupt post-peak behaviour indicates a quasi-brittle fracture mechanism governed mainly by interfacial debonding between the Al_2O_3 grains and Cu particles, resulting from limited wettability and weak adhesion between both phases. Similar compression behaviour has been reported for conventionally sintered Al_2O_3 -Cu composites, where failure occurs predominantly by crack propagation along the matrix-metal boundaries rather than transgranular fracture [44]. Compared with graded Al_2O_3 -Cu composites produced by centrifugal slip casting, which exhibit heterogeneous stress distribution due to the metallic phase gradients, the analysed material demonstrates a more uniform deformation process prior to failure. The obtained results confirm that the incorporation of 10 vol.% Cu improves the deformation capability under compressive loading; however, the dominant fracture mode remains controlled by the brittle ceramic matrix and interface-driven crack propagation. [45].

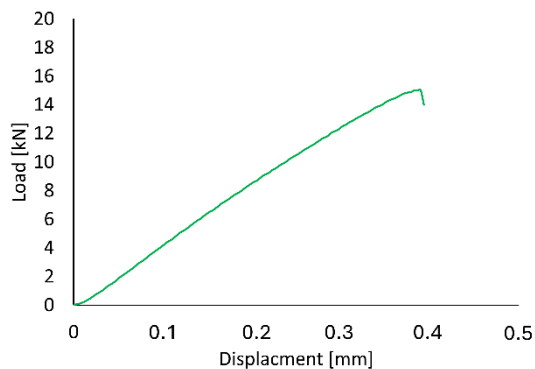


Figure 7. Load versus displacement graph and compressive strength of Al_2O_3 -Cu composite specimens with 10 vol.% metallic phase produced by uniaxial pressing and free sintering in reducing atmosphere.

Figure 8 illustrates the distribution of strains during mechanical loading of the Al_2O_3 -Cu composite containing 10 vol.% Cu, fabricated by uniaxial pressing and free sintering at 1400°C . The strain fields were determined by employing digital image correlation (DIC), enabling full-field analysis of the deformation behavior under compressive loading. At the initial stage of loading, the strain distribution is relatively heterogeneous across the specimen cross-section. Localized zones of elevated effective strain are visible as discrete regions dispersed throughout the material. These strain concentrations are associated with microstructural heterogeneities, including the presence and spatial distribution of the ductile copper phase within the brittle alumina matrix. The metallic inclusions promote local plastic accommodation, leading to nonuniform strain partitioning between the phases. With increasing load, the strain field becomes more pronounced at the specimen boundaries, particularly in the regions adjacent to the loading platen. Elevated strain values are observed near the top and bottom contact areas, indicating stress concentration as a consequence of frictional constraints and limited lateral deformation. The central region of the specimen exhibits comparatively lower strain values at this stage, suggesting that deformation localization precedes macroscopic failure. The final micrograph captures the post-failure state of the specimen, revealing a distinct crack path and fragmentation pattern. The crack appears to originate from regions of high strain concentration and subsequently propagates through the ceramic matrix. The fracture morphology indicates a predominantly brittle failure mechanism, characteristic of alumina-based composites, although the presence of copper likely contributes to limited crack bridging and energy dissipation prior to catastrophic failure.

The strain distribution analysis demonstrates that the Al_2O_3 -Cu composite exhibits heterogeneous deformation behavior governed by phase contrast and interfacial interactions. The incorporation of 10 vol.% Cu influences the strain localization patterns, delaying abrupt failure by enabling partial stress redistribution before crack propagation.

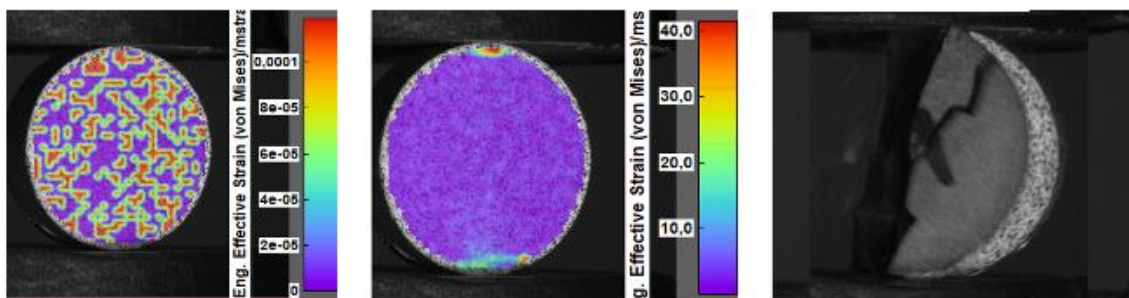


Figure 8. Strain distribution during loading of specimens from Al_2O_3 -Cu system with 10 vol.% metallic phase produced by uniaxial pressing and free sintering at 1400°C .

The microstructural observations obtained by confocal microscopy and SEM clearly demonstrate that the Al_2O_3 -Cu composites exhibit pronounced heterogeneity in the spatial distribution of the metallic phase. Copper is present in irregularly shaped inclusions and agglomerates, leading to regions locally enriched in Cu,

as well as areas where the metallic phase is scarce or absent. This non-uniform distribution is primarily associated with the migration and coalescence of liquid copper during sintering under non-wetting conditions, which promotes the formation of discrete metallic clusters rather than homogeneous dispersion within the ceramic matrix.

This heterogeneity is a key feature of the investigated system. From a microstructural standpoint, the composite should be considered as locally heterogeneous, with significant variation in phase distribution, interfacial area, and local mechanical response. In particular, regions containing larger copper agglomerates are expected to exhibit enhanced plastic accommodation and crack-bridging capability, whereas the Cu-depleted regions are more similar to monolithic alumina, with a limited stress-relaxation capacity.

At the same time, the mechanical response reported in this study, such as hardness or compressive strength, represents a macroscopic, averaged behavior measured over a relatively large volume of material. Therefore, the apparent “homogeneity” of the mechanical properties should be interpreted as an effective response resulting from the statistical averaging of heterogeneous microstructural features. The relatively low scatter in hardness values, for example, reflects the fact that the indentation scale integrates the responses of both phases, even if their local distributions are not perfectly uniform.

However, this does not imply true microstructural uniformity. On the contrary, the observed heterogeneity likely contributes to the variability in properties that are more sensitive to local features, such as fracture toughness, where crack particle interactions strongly depend on the immediate microstructural environment. Similarly, the deformation patterns observed via digital image correlation (DIC) confirm the non-uniform strain localization, consistent with the heterogeneous phase distribution.

It can be assumed that the apparent discrepancy between microstructural heterogeneity and the relatively uniform macroscopic mechanical response arises from differences in the observation scale. The composite exhibits a heterogeneous microstructure at the microscale, while its bulk mechanical properties reflect an averaged response. This distinction is essential for correct interpretation of the results.

Figure 9 presents the grain size distribution of the Al_2O_3 matrix in the Al_2O_3 -Cu composite containing a 10 vol.% metallic phase. The distribution was determined based on quantitative image analysis of the microstructural observations, with grain size expressed as the equivalent circle diameter (d_2). The histogram indicates a predominantly fine-grained microstructure with unimodal distribution. The majority of the Al_2O_3 grains are concentrated within the range of approximately 0.6 - 1.2 μm , with the highest frequency observed around 0.8 - 1.0 μm . Grain sizes below 0.5 μm and above 1.5 μm occur with significantly lower frequency, indicating limited abnormal grain growth during sintering. The relatively narrow distribution suggests that sintering at 1400°C promoted effective densification while maintaining microstructural stability of the ceramic matrix. The absence of a pronounced tail toward larger grain sizes implies that exaggerated grain growth was effectively suppressed, which may be associated with the presence of the dispersed copper phase. The metallic inclusions can act as microstructural pinning points, locally inhibiting grain boundary migration and

contributing to grain growth control. The obtained grain-size distribution confirms that the Al_2O_3 -Cu composite retains a fine, relatively homogeneous ceramic matrix despite the high sintering temperature. Such a microstructural feature is beneficial for maintaining high hardness while enhancing fracture toughness by synergistic interaction between the fine alumina grains and the ductile copper phase.

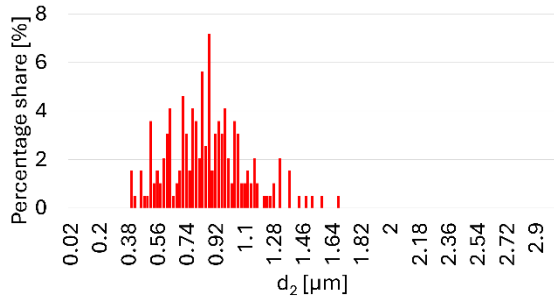


Figure 9. Al_2O_3 grain size distribution in specimens from Al_2O_3 -Cu system with 10 vol.% metallic phase.

Conclusions

This study investigated the fabrication, microstructure, physical properties, and mechanical performance of Al_2O_3 -Cu ceramic-metal composites containing 10 vol.% copper, produced by uniaxial pressing followed by free sintering in a reducing atmosphere. The primary objective was to evaluate the feasibility of manufacturing dense, structurally stable composites using an industrially scalable, cost-effective processing route, despite the challenges posed by the non-wetting behavior of copper in contact with alumina.

Four series of composites were produced and sintered at temperatures ranging from 1200°C to 1400°C . A clear correlation between the sintering temperature and densification was observed. The relative density increased systematically with temperature, reaching 97.32% of the theoretical density at 1400°C . This improvement was accompanied by a substantial reduction in open porosity (down to 0.15%) and water absorption (0.04%), indicating nearly complete pore elimination at the highest temperature. These results demonstrate that effective densification of Al_2O_3 -Cu composites can be achieved via conventional free sintering, provided an appropriate thermal regime is applied.

Phase analysis by X-ray diffraction confirmed the presence of only α - Al_2O_3 and metallic Cu in all the specimens, with no detectable secondary phases or reaction products. Importantly, no relationship was observed between the sintering temperature and phase composition, indicating the system's chemical stability under the applied processing conditions.

Microstructural observations revealed that copper forms irregular agglomerates within the alumina matrix due to liquid-phase migration during sintering. Although the composite exhibited regions of locally increased metallic concentration, no macroscopic copper exudation or surface segregation was observed, suggesting effective capillary retention of the liquid copper within the ceramic skeleton. SEM-EDS analysis

confirmed a two-phase structure with sharp phase boundaries and no evidence of interdiffusion or reaction layers at the Al_2O_3 -Cu interface.

Mechanical characterization of the optimally sintered composite (1400°C) showed a Vickers hardness of 11.7 ± 0.9 GPa and an indentation fracture toughness of 5.90 ± 1.80 $\text{MPa}\cdot\text{m}^{0.5}$, indicating a balanced combination of hardness and improved damage tolerance relative to monolithic alumina. The compressive strength was determined to be 103.26 MPa at a displacement of approximately 0.4 mm. Full-field strain analysis by means of digital image correlation revealed heterogeneous deformation behavior governed by phase distribution and interfacial interactions. Strain localization occurred preferentially near the metallic inclusions and the specimen boundaries, while the failure remained predominantly brittle, characteristic of alumina-based systems, with partial stress redistribution enabled by the ductile copper phase.

Grain size analysis of the Al_2O_3 matrix demonstrated a fine-grained, unimodal distribution with limited abnormal grain growth, even at 1400°C. The presence of copper inclusions likely contributed to grain growth control via local pinning, thereby supporting microstructural stability during high-temperature sintering.

The results confirm that dense and mechanically reliable Al_2O_3 -Cu composites containing a 10 vol.% metallic phase can be successfully fabricated by uniaxial pressing and free sintering. The study provides a comprehensive correlation between the processing parameters, densification behavior, microstructure evolution, and mechanical response. From a materials engineering standpoint, the work demonstrates that a conventional, scalable powder metallurgy route can yield multifunctional ceramic–metal composites with a controlled microstructure and predictable performance, thereby offering a practical potential for structural and shielding applications.

Acknowledgment

The studies were funded by the Faculty of Material Science and Engineering, Warsaw University of Technology, within the framework of research subvention – Project Manager: Ph.D. Eng. Justyna Zygmuntowicz.

References

- [1] Zheng Y., Wu X., Liu L., Sun J., Ning S. Functionally gradient Al_2O_3 ceramics with tailored high-entropy carbide hardening phase and ZrO_2 toughening phase. *J Am Ceram Soc.* 2026;109:e70372. <https://doi.org/10.1111/jace.70372>
- [2] Abyzov A.M. Aluminum oxide and alumina ceramics (review). Part 1. Properties of Al_2O_3 and commercial production of dispersed Al_2O_3 *Refract Ind Ceram.* 2019;60:24–32. [https://doi.org/10.1007/s11148-019-00304-](https://doi.org/10.1007/s11148-019-00304-2)

- [3] Yolshina L.A., Kvashnichev A.G., Vichuzhanin D.I., Smirnova E.O. Mechanical and thermal properties of aluminum matrix composites reinforced by in situ Al_2O_3 nanoparticles fabricated via direct chemical reaction in molten salts. *Appl Sci.* 2022;12(17):8907. <https://doi.org/10.3390/app12178907>
- [4] Su H., Gao W., Feng Z., Lu Z. Processing, microstructure and tensile properties of nano-sized Al_2O_3 particle reinforced aluminum matrix composites. *Mater Des.* 2012;36:590–596. <https://doi.org/10.1016/j.matdes.2011.11.015>
- [5] Chen Y., Ud-din R., Yang T., Li T., Li C., Chu A., Zhao Y. Preparing and wear-resisting property of $\text{Al}_2\text{O}_3/\text{Cu}$ composite material enhanced using novel in situ generated Al_2O_3 nanoparticles. *Materials.* 2023;16(13):4819. <https://doi.org/10.3390/ma16134819>
- [6] Miranda-Hernández J.G., Moreno-Guerrero S., Soto-Guzmán A.B., Rocha-Rangel E. Production and characterization of $\text{Al}_2\text{O}_3\text{-Cu}$ composite materials. *J Ceram Process Res.* 2006;7(4):311–314. <https://doi.org/10.36410/jcpr.2006.7.4.311>
- [7] Jiang C., Liu Z.K., Qin D., Liu T., Zhang X.H., Zeng L.F., Zhao W.M., Liu B.X., Zhang L.N. Preparation and microstructure of $\text{Cu-Al}_2\text{O}_3$ composites by a novel supercritical water liquid phase in-situ reaction method. *Mater Today Commun.* 2024;39:108983. <https://doi.org/10.1016/j.mtcomm.2024.108983>
- [8] Somlyai-Sipos L., Janovszky D., Sycheva A., Baumli P. Investigation of the melting point depression of copper nanoparticles. *IOP Conf Ser Mater Sci Eng.* 2020;903:012002. <https://doi.org/10.1088/1757-899X/903/1/012002>
- [9] Yang Y.W., Cristino V.A.M., Tam L.M., Lo K.H., Kwok C.T. Laser surface alloying of copper with Cr/Ti/CNT for enhancing surface properties. *J Mater Res Technol.* 2022;17:560–573. <https://doi.org/10.1016/j.jmrt.2021.12.129>
- [10] Barakat W.S., Habba M.I.A., Ibrahim A., Fathy A., Elkady O.A. The effect of Cu-coated Al_2O_3 particle content and densification methods on the microstructure and mechanical properties of Al matrix composites. *J Mater Res Technol.* 2023;24:6908–6922. <https://doi.org/10.1016/j.jmrt.2023.05.010>
- [11] Keramat E., Hashemi B. Modelling and optimizing the liquid phase sintering of alumina/ $\text{CaO-SiO}_2\text{-Al}_2\text{O}_3$ ceramics using response surface methodology. *Ceram Int.* 2021;47(3):3159–3172. <https://doi.org/10.1016/j.ceramint.2020.09.153>
- [12] Ravishankar N., Carter C.B. Migration of alumina grain boundaries containing a thin glass film. *Acta Mater.* 2001;49(11):1963–1969. [https://doi.org/10.1016/S1359-6454\(01\)00098-2](https://doi.org/10.1016/S1359-6454(01)00098-2)
- [13] German R.M., Suri P., Park S.J. Review: liquid phase sintering. *J Mater Sci.* 2009;44:1–39. <https://doi.org/10.1007/s10853-008-3008-0>

- [14] Kholodkova A.A., Korniyushin M.V., Khrustalev A.N., Arbanas L.A., Smirnov A.V., Ivakin Y.D. The direct cold sintering of α -Al₂O₃ ceramics in a pure water medium. *Ceramics*. 2024;7(3):1030–1042. <https://doi.org/10.3390/ceramics7030067>
- [15] Xu L., Gao Q., Tang L., Yao Y., Sun S., Li C. Numerical simulation study on hot pressing of ceramic/metal powders. *Mater Today Commun.* 2024;40:109721. <https://doi.org/10.1016/j.mtcomm.2024.109721>
- [16] Zou C., Ou Y., Zhou W., Li Z., Zheng P., Guo X. Microstructure and properties of hot pressing sintered SiC/Y₃Al₅O₁₂ composite ceramics for dry gas seals. *Materials*. 2024;17(5):1182. <https://doi.org/10.3390/ma17051182>
- [17] Tunç B., Somunkiran İ., Balci E. Characterization of Cr₃C₂/Ni ceramic–metal composites produced by direct resistance rapid hot pressing method. *Eur Phys J Plus*. 2025;140:569. <https://doi.org/10.1140/epjp/s13360-025-06502-x>
- [18] Hutsaylyuk V., Student M., Posuvailo V., Student O., Sirak Y., Hvozdet's'kyi V., Maruschak P., Veselivska H. The properties of oxide-ceramic layers with Cu and Ni inclusions synthesizing by PEO method on top of the gas-spraying coatings on aluminium alloys. *Vacuum*. 2020;179:109514. <https://doi.org/10.1016/j.vacuum.2020.109514>
- [19] Hutsaylyuk V., Student M., Posuvailo V., Student O., Hvozdet's'kyi V., Maruschak P., Zakiev V. The role of hydrogen in the formation of oxide-ceramic layers on aluminum alloys during their plasma-electrolytic oxidation. *J Mater Res Technol*. 2021;14:1682–1696. <https://doi.org/10.1016/j.jmrt.2021.07.082>
- [20] Zhou D., Wang X., Muránsky O., Wang X., Xie Y., Yang C., Zhang D. Heterogeneous microstructure of an Al₂O₃ dispersion strengthened Cu by spark plasma sintering and extrusion and its effect on tensile properties and electrical conductivity. *Mater Sci Eng A*. 2018;730:328–335. <https://doi.org/10.1016/j.msea.2018.06.010>
- [21] Shi Y., Chen W., Dong L., Li H., Fu Y. Enhancing copper infiltration into alumina using spark plasma sintering to achieve high performance Al₂O₃/Cu composites. *Ceram Int*. 2018;44(1):57–64. <https://doi.org/10.1016/j.ceramint.2017.09.062>
- [22] Momot K., Klimczyk P., Leszczyńska-Madej B., Podsiadło M., Rumiantseva Y., Gubernat A. From powders to performance-A comprehensive study of two advanced cutting tool materials sintered with pressure assisted methods. *Materials*. 2025;18(2):461. <https://doi.org/10.3390/ma18020461>
- [23] Ejiofor J.U., Reddy R.G. Characterization of pressure-assisted sintered Al-Si composites. *Mater Sci Eng A*. 1999;259(2):314–323. [https://doi.org/10.1016/S0921-5093\(98\)00907-1](https://doi.org/10.1016/S0921-5093(98)00907-1)

- [24] Li S., Chen B., Sun Y., Wang Y., Xie K., Chen X. Experimental and numerical study on the mechanical properties of alumina ceramics based on a modified SHPB setup. *Ceramics*. 2026;9(2):25. <https://doi.org/10.3390/ceramics9020025>
- [25] Momohjimoh I., Hussein M.A., Al-Aqeeli N. Recent advances in the processing and properties of alumina-CNT/SiC nanocomposites. *Nanomaterials*. 2019;9(1):86. <https://doi.org/10.3390/nano9010086>
- [26] Maj J., Węglewski W., Bochenek K., et al. A comparative study of mechanical properties, thermal conductivity, residual stresses, and wear resistance of aluminum-alumina composites obtained by squeeze casting and powder metallurgy. *Metall Mater Trans A*. 2021;52:4727–4736. <https://doi.org/10.1007/s11661-021-06401-7>
- [27] Whitney D. Ceramic cutting tools. In: Sarin V.K., ed. *Comprehensive Hard Materials*. Elsevier; 2014:491–505. <https://doi.org/10.1016/B978-0-08-096527-7.00037-4>
- [28] Ouyang Y., Bai L., Tian H., Li X., Yuan F. Recent progress of thermal conductive polymer composites: Al₂O₃ fillers, properties and applications. *Compos Part A Appl Sci Manuf*. 2022;152:106685. <https://doi.org/10.1016/j.compositesa.2021.106685>
- [29] Žmak I., Čorić D., Mandić V., Čurković L. Hardness and indentation fracture toughness of slip cast alumina and alumina-zirconia ceramics. *Materials*. 2020;13(1):122. <https://doi.org/10.3390/ma13010122>
- [30] Zhang F., Zhao Y., Tian J., Qin B., Dong E., Zhang S., Dong C. Fabrication and characterization of in-situ polymer derived ceramics reinforced copper matrix composites. *Compos Part B Eng*. 2025;307:112873. <https://doi.org/10.1016/j.compositesb.2025.112873>
- [31] Konopka K., Maj M., Kurzydłowski K.J. Studies of the effect of metal particles on the fracture toughness of ceramic matrix composites. *Mater Charact*. 2003;51(5):335–340. <https://doi.org/10.1016/j.matchar.2004.02.002>
- [32] Jiang Z., Sheng G., Li X., Li Y., Xu Z., Guo J., Yin Z., Yin J., Sun Q. Additive manufacturing of triply periodic minimal surface (TPMS) structured dual-coated diamond/copper composites for high performance. *Addit Manuf Front*. 2025;200272. <https://doi.org/10.1016/j.amf.2025.200272>
- [33] Shackelford J.F., Han Y.H., Kim S., Kwon S.H. *CRC Materials Science and Engineering Handbook*. Boca Raton: CRC Press; 2016. <https://doi.org/10.1201/9781315273128>
- [34] Fouda A., Ahmadian H., Nureldeen W., et al. A critical review of copper-graphene nanocomposites: From processing to tribological applications. *Int J Precis Eng Manuf*. 2026. <https://doi.org/10.1007/s12541-025-01415-2>

- [35] Jheng L.C., Wang Y.Z., Huang W.Y., Ho K.S., Tsai C.H., Huang C.T., Tsai H.S. Melting and recrystallization of copper nanoparticles prepared by microwave-assisted reduction in the presence of triethylenetetramine. *Materials*. 2020;13(7):1507. <https://doi.org/10.3390/ma13071507>
- [36] Piotrkiewicz P., Zygmontowicz J., Wachowski M., Cymerman K., Kaszuwara W., Więclaw-Midor A. Al₂O₃-Cu-Ni composites manufactured via uniaxial pressing: Microstructure, magnetic, and mechanical properties. *Materials*. 2022;15(5):1848. <https://doi.org/10.3390/ma15051848>
- [37] Zygmontowicz J., Falkowski P., Miazga A., Konopka K. Fabrication and characterization of ZrO₂/Ni composites. *J Aust Ceram Soc*. 2018;54(4):655–662. <https://doi.org/10.1007/s41779-018-0194-3>
- [38] Lis J., Pampuch R. *Spiekanie*. Kraków: AGH Uczelniane Wydawnictwa Naukowo-Dydaktyczne; 2000. <https://doi.org/10.13140/RG.2.1.1234.5678>
- [39] Gizowska M., Miazga A., Konopka K., Szafran M. The influence of sintering temperature on properties of Al₂O₃-Ni composites. *Compos Theory Pract*. 2012;12(1):33–38. <https://doi.org/10.5604/20843867.1000000>
- [40] Lankford J. Indentation microfracture in the Palmqvist crack regime: Implications for fracture toughness evaluation by the indentation method. *J Mater Sci Lett*. 1982;1(11):493–495. <https://doi.org/10.1007/BF00721938>
- [41] Wejrzanowski T., Kurzydłowski K.J. Stereology of grains in nanocrystals. *Solid State Phenom*. 2003;94:221–228. <https://doi.org/10.4028/www.scientific.net/SSP.94.221>
- [42] Michalski J., Wejrzanowski T., Pielaszek R., Konopka K., Łojkowski W., Kurzydłowski K.J. Application of image analysis for characterization of powders. *Mater Sci Poland*. 2005;23:79–86. <https://doi.org/10.2478/v10006-008-0003-1>
- [43] Wejrzanowski T., Spychalski W., Roźniatowski K., Kurzydłowski K. Image-based analysis of complex microstructures of engineering materials. *Int J Appl Math Comput Sci*. 2008;18(1):33–39. <https://doi.org/10.2478/v10006-008-0003-1>
- [44] Piotrkiewicz P., Zygmontowicz J., Wachowski M., Szachogłuchowicz I., Kaszuwara W. Influence of the second metal component on processing and selected properties of Al₂O₃-Cu hybrid composites. *Processing and Application of Ceramics* 2024;18(1):98–108. DOI: 10.2298/PAC2401098P
- [45] Wachowski M., Kaszuwara W., Miazga A., Konopka K., Zygmontowicz J., The possibility of producing graded Al₂O₃-Mo, Al₂O₃-Cu, Al₂O₃-W composites using CSC method. *Bulletin of the Polish Academy of Sciences Technical Sciences* 2019;67(2). DOI: 10.24425/bpas.2019.128603